

THE USE OF OPTICAL METHODS IN THE ANALYSIS OF THE AREAS WITH STRESS CONCENTRATION

PÁSTOR Miroslav¹, FRANKOVSKÝ Peter¹,
HAGARA Martin¹, LENGVARSKÝ Pavol¹

¹Technical University of Košice, Faculty of Mechanical Engineering, Department of Applied Mechanic and Mechanical Engineering, Letná 9, 042 00 Košice, Slovak Republic, email: miroslav.pastor@tuke.sk

Abstract: Anchoring parts of technical systems are often damaged due to the heavy forces acting on these systems during their operation. For that reason, various modifications are suggested and created on the anchoring screws, which should help to reduce the mechanical stress values in a place of the first load-bearing thread of a female screw. For the determination of stress fields on the surface of a plane model of a threaded joint, two non-contact optical methods were used – conventional transmission photoelasticimetry and modern digital image correlation.

KEYWORDS: Nondestructive testing, Digital image correlation, Optical systems

1 Introduction

The influence of a notch effect on the threaded joints belongs to the most important, as well as the most negative, features occurring during fatigue loading of constructions and machines. In a case of a screw and a female screw (Fig. 1) at the transition of cylindrical part of screw into head (area A), a thread run-out (area B), a thread (area C) and a thread of screw in a place of the first load-bearing thread of a female screw (area D), belong to the crucial construction notches.

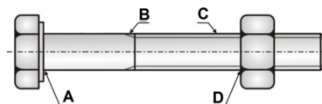


Fig. 1 The areas of the construction notches in a threaded joint.

In areas of the construction notches, stress concentration occurs. At static loading, it is characterized by the theoretical shape stress factor α_σ , which is defined as a ratio between the maximal stress in a place of the notch and the nominal stress. Thread (area C) is represented by a number of subsequent notches, so the stress concentration factor is smaller than that occurring in one notch of the same shape, because the neighboring notches decrease the local curving of the tension stress field lines.

The biggest notch factor, β_σ , occurs in the screw thread, in the place D. It is caused by the stress distribution in the screw thread, which is markedly changing in a part of the thread cooperating with the first threads of the female screw. The change of stress distribution is evoked by a non-uniform force distribution appearing in particular threads of the screw (Fig. 2), due to a different deformation of the screw and the female screw. The first thread of the female screw and its corresponding screw cross-section is loaded the most. This results in the biggest notch effect, occurring in the first load-bearing thread, caused by a loading from a force flow in the screw shank as well as a local bending of the most loaded mentioned thread. According to

Fig. 2, the first female screw thread transmits approximately 1/3 of loading force and the notch factor is of a value from 4 up to 8. Moreover, a plastic deformation as well as an impression of the first meshing threads of the screw and the female screw can appear upon tightening of the female screw with a higher tightening torque [1].

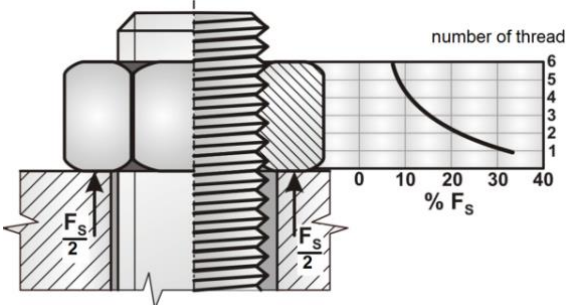


Fig. 2 Non-uniform distribution of forces in the female screw threads.

The notch factor β_σ for a screw thread, is dependent on the mechanical properties of a screw, the technology of its manufacturing, the face, the shape of a thread profile, the type and the height of the female screw. To ensure the minimal value of the notch effect in a normalized thread, it is necessary to decrease the relative loading of the first and the second thread and to ensure the best quality of its face next to its profile root. An increased threaded joint fatigue strength can be realized by some constructional modifications, which result from the change of the female screw deformation strength in a surrounding of the first threads in such a way, that its cross-section area is decreased and the conditions for its bending opening are thus created. For illustration, we introduce three loaded threads with decreased stress caused by the constructional modification of the female screw. A creation of the notch in a female screw causes a decreasing of the stress in its first threads as well as an increasing of the stress in the other ones, loaded by a lower force.

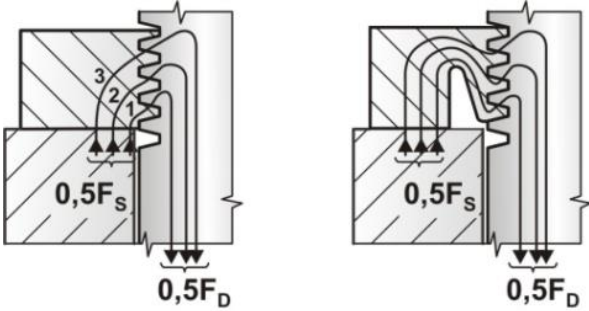


Fig. 3 The force flow distribution occurring in a female screw without modification (left) and with a notch (right).

Fig. 4 displays a prototype of the female screw M56 with a created notch, which the authors used for the anchoring of a large metallurgical system [2, 3].

During operational loading in a real threaded joint, a triaxial state of stress occurs. Currently, the numerical modeling methods are used most frequently for stress analyses in the areas with a high stress gradient. However, they are relatively challenging in regard to a correct definition of the boundary conditions. For the experimental examination of a suitability of the suggested constructional modification, the authors used a simplified thread joint model, which does not consider tangential stress. The aim of the proposed methodology should be a verification of the results obtained by the finite element method via the optical methods of mechanics.



Fig. 4 Female screw M56 with a created notch used for anchoring of a casting pedestal.

2 Stress analysis using transmission photoelasticity

Transmission photoelasticimetry is an optical method suitable for the stress fields' analyses of the optically sensitive models at a static or a dynamic loading. By transmission photoelasticimetry, the measurement is realized using a light falling perpendicularly on the surface of optically sensitive plate. The stress distribution can be observed via analyzer by an analysis of the color fringes, which provide some prompt information about their full allocation as well as of the areas of high stress gradient. A quantitative stress analysis can be performed with optical compensator attached to a polariscope. For the experimental investigation a polariscope Model 060 from Measurements Group, Inc., was used. Besides a realization of accurate measurements of stress in chosen locations, this type allows also wide range of applications within a full-field stress analysis. It can be used for a prompt determination of nominal stress, stress gradients and general stress distribution, including identification of overloaded and lightly loaded areas. A successful application of this characteristic known as a full-field interpretation is dependent on a recognition of isochromatic fringe order according to the color and the understanding of the relation between a fringe order and a stress amount. General photoelastic patterns commonly signify the necessity of corrective steps for a prevention against failure and pursuant to them, some material from the investigated object is often removed and thus its weight is reduced. A full-field image of stress distribution can identify the overloaded areas indicating a failure. On the other hand, there are some areas with nearly zero stress. Small changes in an object shape allow stress redistribution that eliminates the stress concentration, whereby a part of loading is transmitted from the overloaded to the lightly loaded areas. The photoelasticimetry provides to erudite experts some general information unreachable by blind stress measurement in a point [4-6].

During measurement, a photoelastic model is located in a working space of a polariscope and as a result of an action of force, the color fringes are observed (Fig. 5).

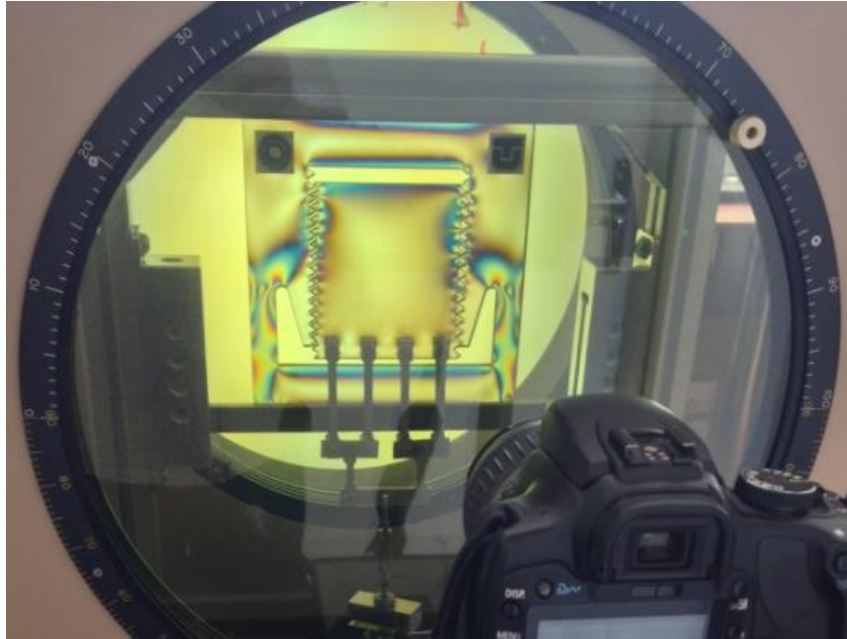


Fig. 5 The view on a photoelastic model in a working space of the polariscope.

These fringes visualize the stress distribution along the whole model surface. The polariscope allows the following analyses or measurements:

- a full-field interpretation of the fringe patterns allowing general valuation of the amounts of nominal stress and stress gradients;
- a quantitative measurement of:
 - the principal stress directions;
 - the values and the signs of the shear stress along free (unloaded) edges and in the areas of uniaxial stress state;
 - the values of the principal stress difference in the case of a plane stress state.

If the photoelastic model is loaded, the principal stresses create an adequate optical effect, which is manifested by the creation of the isochromatic fringes. Observed fringe order is adequate to principal stress difference. This linear dependence can be described by the relation

$$\sigma_1 - \sigma_2 = \frac{NC}{t}, \quad (1)$$

where N is the fringe order (observed birefringence), C is the stress-optical constant of a material of the model, t is the thickness of a model and σ_1, σ_2 are the principal stresses.

Equation (1) for the shear stress can be expressed in a form

$$\tau_{\max} = \frac{1}{2} \frac{NC}{t}, \quad (2)$$

where τ_{\max} is the maximal shear stress (acting in a plane perpendicular to the model plane) in an appropriate point.

It is essential that the value of principal stress difference or the value of maximal shear stress in the model can be simply obtained by the determination of fringe order and its multiplication by Ct^{-1} . In technical practice, there are a lot of cases, when it is obvious that the stress state is uniaxial with the zero stress σ_1 , or σ_2 . On the edge of the specimen, one of the principal stresses is always non-zero and can be calculated directly from Eq. (1).

For a two-dimensional model analysis of a plane state of stress, an optically sensitive material, the PSM-1 was chosen. It is a polycarbonate material, which is tough, easily processable and has an excellent transparency. It is suitable for manufacturing of models without creep or edge effect and with a very good photoelastic optical sensibility. The properties of the used PSM-1 material are present in Table 1.

Table 1. Properties of an optically sensitive material, the PSM-1.

Stress-optical constant C [kPa/fringe/m]	7.0
Young modulus E [GPa]	2.5
Poisson ratio μ	0.38
Thickness t [mm]	9.5

By a sequential loading of the model, the color fringes (isochromatics) appear in locations with high stress levels and expand to the locations with low stress levels. Isochromatics are the geometrical locations of points, along which the difference of the principal stresses (σ_1, σ_2) remains constant.

Table 2. Characteristics of the isochromatics of the PSM-1 material.

Color	Approximate relative delay [mm]	Fringe order	Stress [MPa]
black	0	0	0
grey	160	0.28	0.21
white	260	0.45	0.33
sallow	345	0,60	0.44
orange	460	0,80	0.59
red	520	0.90	0.66
purple	575	1.00	0.74
dark blue	620	1.08	0.80
blue-green	700	1.22	0.90
green-yellow	800	1.39	1.02
orange	935	1.63	1.20
pink-red	1050	1.82	1.34
purple	1150	2,00	1.47
green	1350	2.35	1.73
green-yellow	1440	2.50	1.84
red	1520	2.65	1.95
red-green	1730	3.0	2.21
green	2400	4.15	3.06

When using a specified achromatic light, the photoelastic fringes appear as a series of successive and sequential heterochromatic fringes, in which each fringe represents a different birefringence order. The color of a singular fringe identifies specifically the birefringence or the fringe order (the stress level) along this fringe. In case we accept the stability of the order in which the colors appear, for a visualization of the stress distribution, the photoelastic fringe pattern can be read like a topographic map. The fringe patterns are caused by the change of a constructive and a destructive interference between the light beams with a delay or a phase shift in the photoelastic model. The transition values of relative delay produce the transition values of light intensity. The specified achromatic light, in general used for the full-field interpretation of fringe patterns, consists of all the wave lengths of the visible spectrum. The relative delay, which causes a decay of one wave length (color), in general does not inhibit the others. In case each color in the spectrum is gradually inhibited according its wave length, due

to the increasing birefringence, the examiner can observe an additional color. The entire color order for the PSM-1 material with a thickness of 9.5 mm is presented in Table 2., whereby for each color, the relative delay as well as the fringe order, is introduced.

For the stress analysis, it was necessary to design a simplified model of the threaded joint, which corresponds as much as possible, to the real conditions and can be used for experimental investigation using optical methods. The simplified model of the analyzed threaded joint consists of two parts, whereby the essential principles of similarity theory were used for their design. The division of the material was realized via water jet technology, in order to eliminate a possibility of the residual stresses appearing on the model boundaries.

Experimental measurements were realized by a loading of 50 N, 100 N, 150 N, 200 N and 250 N. The value of the loading tension force, acting on the inner part of the model, was recorded via the strain indicator Vishay P3. The outer part of model, presenting the female screw with a notch, was supported in its lower part to prevent its moving by acting of the applied force. A view on the measuring string can be seen in Fig. 6.

Fig. 7a depicts an unloaded model of the threaded joint located in the working space of the polariscope. If the model is loaded and the loading is consequently increased, at first the fringes appear in locations with the maximal stresses (Fig. 7b). During the next increase of a loading force, some new fringes appear and the older ones are transferred to the locations with lower stress (Fig. 7c). After that, the same process is repeated until the state of maximal loading is reached (Fig. 7d).



Fig. 6 Measuring string used by the measurement via transmission photoelasticity.

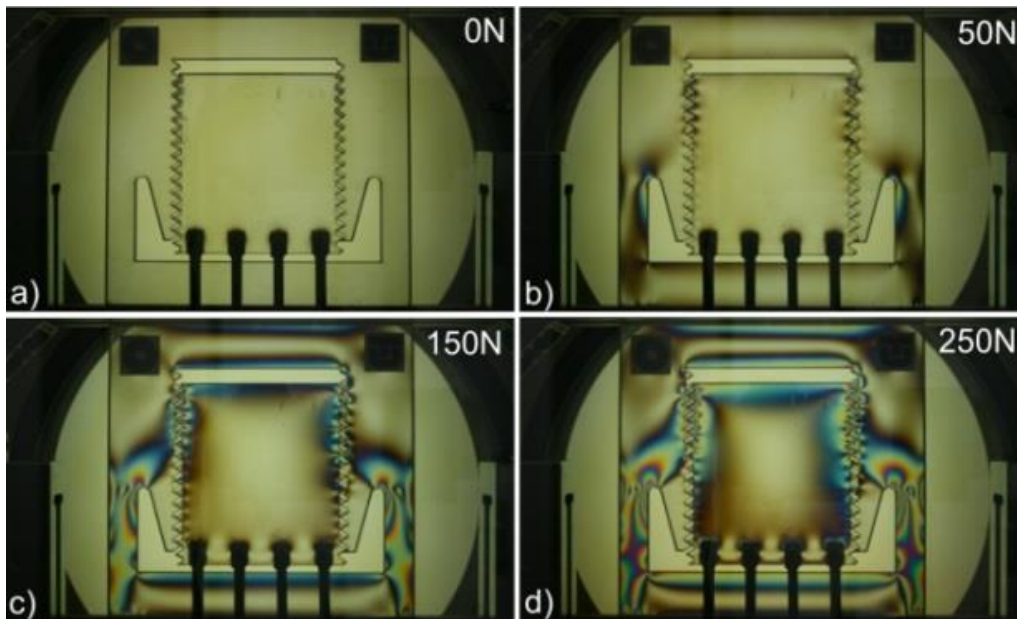


Fig. 7 Formation of the isochromatic fringes on the analyzed model during the increase of the loading force.

From the stress distribution (Fig. 7d), it is clear, that the levels of reduced stresses in a surrounding of the first threads are lower than the stresses observed on the threads of the model gross section, which is due to the creation of the notch. The mentioned increase of stress levels is not dangerous in regard to the safety of the threaded joint. It is also interesting that the stress fields' distribution is not absolutely symmetric. It is caused by the construction of both parts of the threaded joint (a relative displacement between the threads on the left and the right side of the model about one half of the thread height).

The process of stress quantification in a chosen point on the model boundary is depicted in Fig. 8.

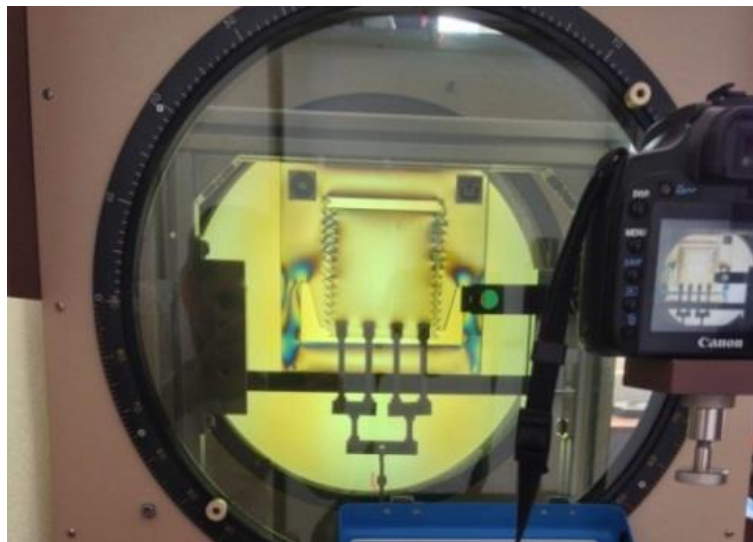


Fig. 8 Readout of the fringe order in the analysed point.

3 Stress analysis using digital image correlation (DIC)

The stress analysis of the plane threaded joint model was also performed using digital image correlation method. The principle of the image correlation systems is based on a comparison of digital images (called correlation), during a loading process of the analyzed object [7-9]. This

comparison is not made on the whole images, but on small image elements called facets. To avoid the correlation of non-corresponding parts, it is necessary to create on the investigated object a surface with a random black and white pattern with high contrast, so that each facet comprises a part of black as well as white color and thus becomes unique.

The correlation systems developed by Dantec Dynamics A/S use for the image correlation an algorithm based on a pseudo-affine transformation. If Fig. 9 visualizes the parameters, $a_0 \dots a_7$ labeled as the transformation parameters of potential displacement, tension, shear or torsion of the object, then according to the mentioned algorithm, the transformation coordinates x^* and y^* can be expressed by the relations

$$\begin{aligned} x^*(a_0, a_1, a_2, a_3, x, y) &= a_0 + a_1x + a_2y + a_3xy, \\ y^*(a_4, a_5, a_6, a_7, x, y) &= a_4 + a_5x + a_6y + a_7xy. \end{aligned} \quad (3)$$

The unknown transformation parameters $a_0 \dots a_7$, can be determined by a minimization of a difference between the grey value of certain point at the deformed image $f(x^*, y^*)$ and the grey value of the same point at the reference image $f(x, y)$ by

$$\min_{a_0, \dots, a_7, a_0, a_1} \sum_{x, y} \|f(x, y) - (g_0 + g_1 \cdot f(x^*(x, y), y^*(x, y)))\|, \quad (4)$$

where g_0 , or g_1 represent the illumination parameters [10].

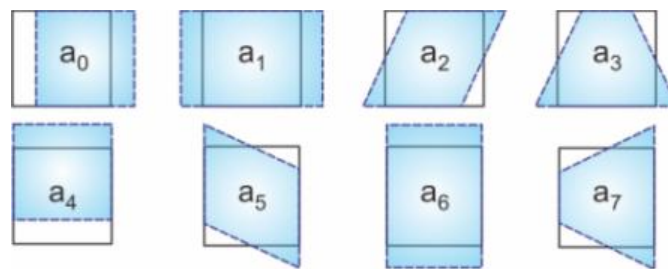


Fig. 9 Transformation parameters.

Analogous to the human vision, by assembling two lightly shifted 2D images, a 3D image is perceived. While the displacements of the object points are determined via a comparison of the object contour during the object loading, the strain is obtained by the analysis of the local facets used in correlation process.

For the measurement, the correlation system Q-400 Dantec Dynamics, consisting of two cameras with the maximal resolution of 5 MPx (2452x2056 px) with the Schneider Kreuznach objective lens, made in Germany, was used. The data transfer to the notebook with the Istra4D control software is ensured by a high-speed serial bus with an IEEE 1394 interface. As the cameras do not dispose of any internal memory, the transfer of the snapshots, directly to the notebook, is made using an external FireWire800 CardBud card with the data transfer speed of 800 Mbit/s. Synchronization of the cameras is ensured by a TU-4XB bus, which the cameras are connected with using coaxial cables with a BNC connector. An output from the software is in a form of the object contour, displacements and strains obtained in each modal point of a so-called virtual grid. A version of the Istra4D program, used for the experimental investigation, does not allow depicting of the stress fields, therefore for their determination, it is necessary to post-process the measured data.

The measurement itself was realized using a two-camera correlation system with the resolution of 2148x2000 px. As the aim was to capture the whole surface of the analyzed specimen, it was necessary to locate the cameras into a distance of ca. 850 mm off the object

surface. An angle, which they form together with the specimen, was set in such a way, that the distortion of lenses was as small as possible (Fig. 10).



Fig. 10 Measuring string used by the measurement via DIC method.

The size of the random speckle pattern, which was printed on a vinyl foil and attached to the object surface, was adjusted to the distance between the cameras and the object, whereby the maximal speckle size was approximately $500\ \mu\text{m}$. Such way of random pattern creation was used and proven in several contributions of the authors, e.g. [11, 12], because the speckle size can be simply adjusted to the measurement conditions and in consideration of the elasticity of the foil, which totally copies the object surface, it is not a problem to perform measurement even in places with plastic deformation. To ensure optimal lighting conditions a powerful source of spotlight was used. The view from one of the cameras, on the analyzed object with created speckle random pattern, can be seen in Fig. 11.

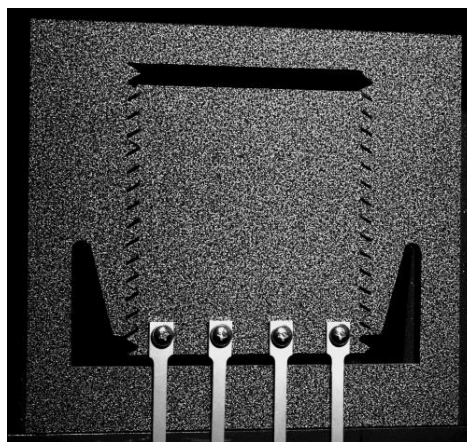


Fig. 11 Object surface with created speckle pattern captured by one of the cameras.

The measurement was realized under the same conditions as by the use of the transmission photoelasticimetry. The specimen was loaded, in sequence, by the tension forces of 50 N, 100 N, 150 N, 200 N and 250 N, whereby the digital images captured during such loading were compared with the one captured in a state without loading. The camera calibration, by which the correlation system gains data about the inner (focal length, principal point location, tangential and radial distortion level) as well as outer (relative location and rotation of the cameras) parameters and can determine the distance from the object and its size but also remove the objective distortion, which is evident also from Fig. 11, was realized by a checkered calibration target with 9×9 black and white fields (Fig. 12), with a size of 11 mm. The facet size used for evaluation was adjusted to the size of the speckles in the random pattern [13]. By the facet size of 11×11 px, the system evaluated approximately 119,000 facets on both images.



Fig. 12 Illustration photo of the Dantec Dynamics calibration targets.

The obtained data were imported into the Q-STRESS v.1.0 program, developed at the authors' department, which allows the calculation and visualization of the stress fields in a form of the normal stresses, the shear stress, the principal stresses as well as according to Guest's Stress, Saint-Venant's Stress and von Mises Stress Theory [14]. In Fig. 13, the Guest's Stress field (corresponding to the difference of the principle stresses obtained by transmission photoelasticimetry by the loading of the inner threaded joint part with tension force 250 N) is depicted.

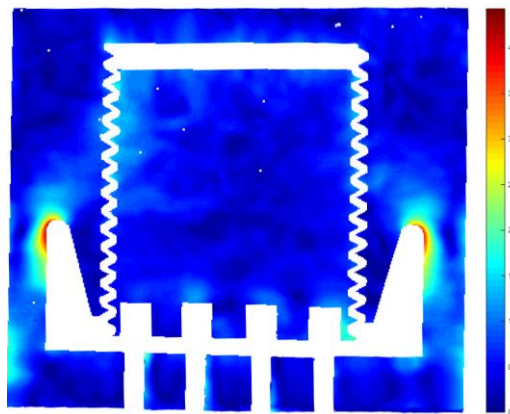


Fig. 13 Field of equivalent Guest stresses on the whole object surface by the loading force of 250 N obtained by digital image correlation.

In order to determinate the values of Guest Stress, as accurately as possible via digital image correlation, it was necessary to use all the cameras' resolution on a smaller part of the specimen. For that reason, the measurement was repeated at the same boundary conditions, however the cameras were located closer to the model (into a distance of ca. 360 mm) and oriented on the area depicted in Fig. 14.



Fig. 14 Image captured by one of the cameras at a detailed analysis of the area with the notch.

As can be seen, also the random speckle pattern created on the object surface was changed to a finer one, to avoid a massive loose of a spatial resolution in the area of the threads, caused by non-adjustment of the speckle size to the facet size.

In this case, the cameras were calibrated using a calibration target with the field of 4 mm size. The facet size was adjusted to the speckle pattern, which was again printed on a vinyl foil, to ensure that each facet comprises a part of black as well as of white color. By the facet size of 15x15 px used for evaluation, 46746 facets were correlated on the analyzed model part.

The Guest Stress field, obtained by the maximal loading using Q-STRESS v.1.0, is depicted in Fig. 15. Although the gap between the threads contact faces is smaller than in the first measurement performed via DIC, neither in this case, they were not completely correlated. The reason is that by the use of two-camera system, the views from cameras are mutually turned by an angle, one from the other. The use of a single camera, with a 2D correlation system and a set very small facet size could be a solution, but still not a perfect one. However, in that case, it is necessary to configure the camera in such a location that its image plane would be parallel with the model surface and ensure the plane strain of the model during its loading. If these conditions are not fulfilled, also a small deviation can cause a significant error in the evaluation process, if the camera is located pretty close to the model, as it is in this case. Appropriate attention should be paid to correlation errors, which increase with a decreasing facet size [15-17].

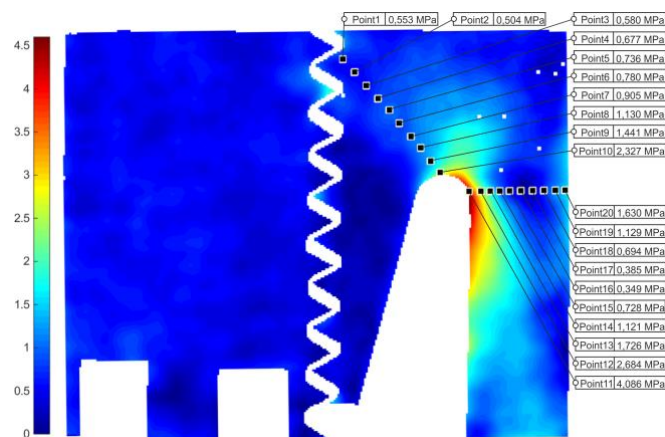


Fig. 15 Field of equivalent Guest stresses obtained in Q-STRESS v.1.0, depicted with the distribution of virtual gages in a surroundings of the notch.

4 Stress analysis using finite element method

A finite element method forms the basis in the design and modelling of the physical phenomena in various engineering disciplines. It is a computer method assigned to the solution of real engineering problems such as stress analysis, vibration analysis, flow, electromagnetic or thermal loading [18 - 20].

By the manufacturing of the real threaded joint model a clearance between the threads of the screw and the female screw appeared due to the use of water jet technology of dividing. For that reason, in the first phase of a numerical modelling, the influence of the clearance between the threads of the screw and the female screw on the results of the stress analysis was assessed. The finite element model with the boundary conditions, equal to these ones used in experimental investigation, was submitted to a static analysis with the loading force of 250 N. By the mentioned analysis, the model was divided into a mesh of finite elements with maximal element size of 6 mm with a refinement in the surroundings of the threads and the notch (Fig. 16). The mesh was thus approximately created by 186 000 elements and 292 000 nodes.

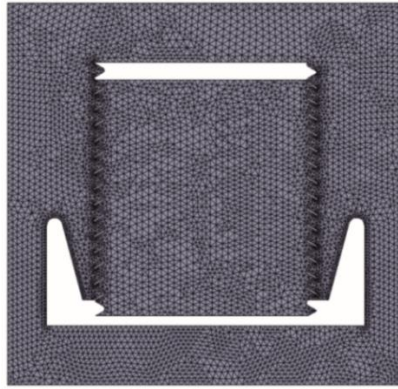


Fig. 16 Finite element mesh created on the numerical model.

From the performed numerical analysis and the results introduced in Fig. 17 and Fig. 18, it is obvious that the clearance between the threads of the screw and the female screw do not influence the stresses, the values of which differ maximally in 1%. The difference in the stress distribution can be observed mainly in the upper part of the notch, where the stress concentration can be found on a bigger area by the use of the model without the clearance.

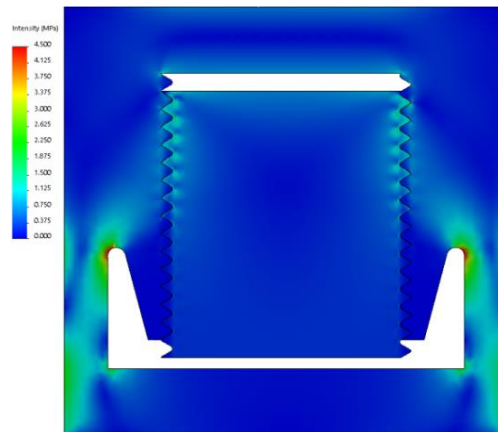


Fig. 17 Field of equivalent Guest stresses on the model surface without clearance.

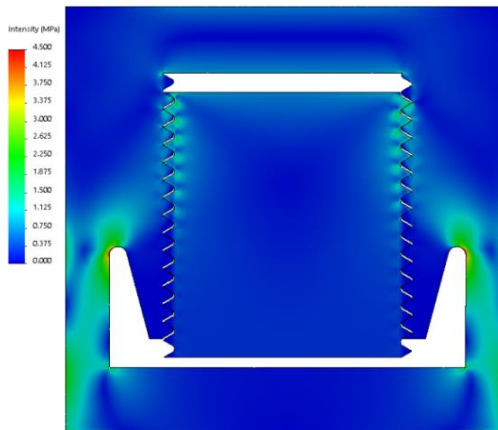


Fig. 18 Field of equivalent Guest stresses on the model surface with clearance.

5 Discussion of the obtained results

A quantitative comparison of the Guest stresses determined by DIC method and FEA was realized in the chosen points, labeled by the numbers from 1 to 20 (see Fig. 15), in which the values of Guest stress, given in Table 3. and Table 4., were acquired. The courses of the mentioned Guest stress values are depicted in Fig. 19 and Fig. 20. The values of Guest stress determined by transmission photoelasticimetry were also compared to the results mentioned

above. The fringe order was read in the locations on the unloaded edge of the model, by a compensator model 032. Using the relation (1) and considering the properties of the PSM-1 material, the following values of Guest stress in point 10 and 20 were obtained

$$\sigma_{10} = 2.29 \text{ MPa,}$$

$$\sigma_{20} = 1.66 \text{ MPa.}$$

It is obvious that for the points 10 and 20, the results acquired by numerical modelling, as well as by experimental investigation, show very good agreement.

Table 3. Guest stress values obtained in points 1-10

Point	DIC [MPa]	FEA [MPa]	Difference [%]
1	0.553	0.527	-4.67
2	0.504	0.478	-5.14
3	0.580	0.551	-5.00
4	0.677	0.643	-5.06
5	0.736	0.696	-5.46
6	0.780	0.741	-5.00
7	0.905	0.864	-4.52
8	1.130	1.083	-4.16
9	1.441	1.415	-1.80
10	2.327	2.227	-4.30

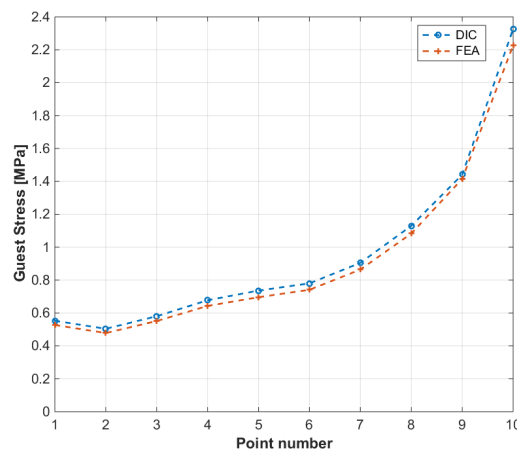


Fig. 19 Course of the Guest stress – points 1-10.

Table 4. Guest stress values obtained in points 11-20

Point	DIC [MPa]	FEA [MPa]	Difference [%]
11	4.086	4.066	-0.49
12	2.684	2.662	-0.82
13	1.726	1.689	-2.12
14	1.121	1.117	-0.34
15	0.728	0.693	-4.78
16	0.349	0.322	-7.79
17	0.385	0.371	-3.66
18	0.694	0.68	-2.02
19	1.129	1.042	-7.71
20	1.630	1.609	-1.29

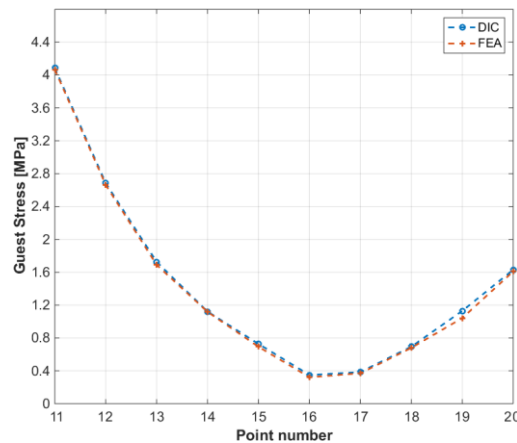


Fig. 20 Course of the Guest stress – points 11-20.

CONCLUSION

The contribution is devoted to a proposal of methodology for the verification of the Guest stress distribution in a simplified model of the threaded joint, using two non-contact optical methods – a transmission photoelasticity and a digital image correlation. In the analyzed model made from optically sensitive material, the notch was created with the aim to relieve the first load-bearing threads of the threaded joint.

The full-field experimental stress analysis confirmed a good agreement with the results acquired by numerical modelling using the finite element method, when the maximal difference between determined Guest stress values was approximately 8 %. Although the transmission photoelasticity method allows relatively rapid summary of the stress distribution on the analyzed specimen surface, the result of the analysis is still in a form of Guest stress. On the other hand, the use of digital image correlation requires longer time, associated with the creation of the necessary random speckle pattern on the object surface, the calibration of cameras and correlation of the images, but it allows visualization of normal stress, shear stress, principal stress as well as reduced stress. The drawback of digital image correlation method is a loss of the spatial resolution in more complicated parts of the contour (concretely in the area of stress concentrators). This problem can be solved using a single camera system with image plane parallel to the object surface (the need for ensuring plane strain) or by the use of the cameras with higher resolution, which allow the correlation of images with optimized facet size.

According to a comparison of the results acquired by experimental and numerical modelling, it can be stated, that the described experimental methods have a practical relevance for constructors and developers mainly from the reason of relatively fast and sufficiently accurate report about the stress fields distribution in components and structures. By the use of basic principles of model similarity, it is possible to transform the results acquired experimentally to real constructions or machines.

Taking into account that the authors' department disposes of extensive equipment for the realization of semi-destructive residual stress analysis and the authors reached in their previous works relatively good results in the area of the stress analysis performed in the surroundings of a small hole [21, 22], their ambition will be a preparation of the methodology for the measurement of residual stresses, using the optical methods of mechanics.

Acknowledgement

This paper was supported by project VEGA No. 1/0751/16 and project ITMS 26220120060 supported by the Research & Development Operational Program funded by the ERDF.

REFERENCES

- [1] F. Trebuňa, F. Šimčák. Stability of the Mechanical System Elements (in Slovak), Košice, **2004**
- [2] F. Trebuňa, F. Šimčák, J. Bocko, M. Pástor. Analysis of the Causes of Casting Pedestal Failures and the Measures for Increasing Their Residual Lifetime. *Engineering Failure Analysis* **2013** (29), 27 – 37.
- [3] F. Trebuňa, et al. Final Report on the Examination of the Anchor Threaded Joints of the ZPO 2 Casting Pedestal (in Slovak). Košice **2014**.
- [4] Y. Nashwan. Experimental Strain Investigation of Bolt Torque Effect in Mechanically Fastened Joints. *Engineering* **2012** (4), 359 – 367.
- [5] M. Fernández. Metrological Study for the Optimal Selection of the Photoelastic Model in Transmission Photoelasticity. *Applied Optics* 2011 (50), No. 29, 5721 – 5727.
- [6] M. Pástor, F. Trebuňa. Application of Transmission Photoelasticity for Stress Concentration Analyses in Construction Supporting Parts. *Applied Mechanics and Materials* **2014** (611), 443 – 449.
- [7] A. Mudassar, S. Butt. Improved Digital Image Correlation for In-plane Displacement Measurement. *Applied Optics* **2014** (53), No. 5, 960 – 970.
- [8] C. Quan, J. Tay, W. Sun, X. He. Determination of Three-dimensional Displacement Using Two-dimensional Digital Image Correlation. *Applied Optics* **2008** (47), No. 4, 583 – 593.
- [9] T. Fricke-Begemann. Three-dimensional Deformation Field Measurement with Digital Speckle Correlation. *Applied Optics* **2003** (42), No. 34, 6783 – 6796.
- [10] T. Siebert, T. Becker, K. Splitthof. Analysis of Advanced Materials under Load. SPIE – The International Society for Optical Engineering, **2006**.
- [11] M. Hagara, M. Schrötter, P. Lengvarský. Influence of the Different Random Pattern Creation Forms on the Results of Experimental Modal Analysis Performed by High-speed Digital Image Correlation. *Acta Mechanica et Automatica* **2014** (8), No. 1, 22 – 26.
- [12] M. Schrötter, M. Hagara, M. Kalina. The Analysis of Different Stochastic Patterns during Loading in Plastic Area Using the DIC Method. *Applied Mechanics and Materials* **2014** (611), 490 – 495.
- [13] B. Pan, H. Xie, Z. Wang, K. Qian, and Z. Wang. Study on Subset Size Selection in Digital Image Correlation for Speckle Patterns. *Optics Express* **2008** (16), No. 10, 7037 – 7048.
- [14] M. Hagara, R. Huňady. Q-STRESS v.1.0 – a Tool for Determination of Stress Fields Using Digital Image Correlation Systems. *Procedia Engineering* **2014** (96), 136 – 142.
- [15] T. Becker, K. Splitthof, T. Siebert, P. Kletting. Error Estimations of 3D Digital Image Correlation Measurements. Technical note, *Dantec Dynamics*, **2008**.
- [16] T. Siebert, T. Becker, K. Splitthof, I. Neumann, R. Krupka. Error Estimations in Digital Image Correlation Technique. *Applied Mechanics and Materials* **2007** (7-8), 265 – 270.
- [17] H. W. Schreier, M. A. Sutton. Systematic Errors in Digital Image Correlation Due to Undermatched Subset Shape Functions. *Experimental Mechanics* **2002** (42), 303 – 310.

- [18] A. Choudhury, C.M. Samar and S. Susenjit. Effect of Lamination Angle and Thickness on Analysis of Composite Plate Under Thermo Mechanical Loading. *Journal of Mechanical Engineering – Strojnícky časopis* **2017** (67), No. 1, 5 – 22.
- [19] M. Pástor and P. Lengvarský, "Analysis of stress and deformation fields of shape complex beams", MATEC Web Conf. 157 02037 (2018)
- [20] R. Čech, P. Horyl P. Maršálek. Modelling of Two-Seat Connection to the Frame of Rail Wagon in Terms of Resistance at Impact Test. *Journal of Mechanical Engineering – Strojnícky časopis* **2016** (66), No. 2, 101 – 106.
- [21] M. Hagara, R. Huňady, F. Trebuňa. Stress Analysis Performed in the Near Surrounding of a Small Hole by a Digital Image Correlation Method. *Acta Mechanica Slovaca* **2014** (18), No. 3 – 4, 74 – 81.
- [22] P. Frankovský et al. Utilization Possibilities of PhotoStress Method in Determination of Residual Stresses. *Applied Mechanics and Materials* **2015** (732), 3 – 8.